GRP78 haploinsufficiency suppresses acinar-to-ductal metaplasia, signaling, and mutant *Kras*-driven pancreatic tumorigenesis in mice

Jieli Shen[a], Dat P. Ha[a], Genyuan Zhu[a], Daisy F. Rangel[a], Agnieszka Kobielak[a,1], Parkash S. Gill[b], Susan Groshen[c], Louis Dubeau[b], and Amy S. Lee[a,2]

[a]Department of Biochemistry and Molecular Biology, University of Southern California Norris Comprehensive Cancer Center, Keck School of Medicine, University of Southern California, Los Angeles, CA 90089-9176; [b]Department of Pathology, University of Southern California Norris Comprehensive Cancer Center, Keck School of Medicine, University of Southern California, Los Angeles, CA 90089-9176; and [c]Department of Preventive Medicine, University of Southern California Norris Comprehensive Cancer Center, Keck School of Medicine, University of Southern California, Los Angeles, CA 90089-9176

Edited by David A. Cheresh, University of California, San Diego, La Jolla, CA, and accepted by Editorial Board Member Peter K. Vogt April 7, 2017 (received for review September 28, 2016)

Pancreatic ductal adenocarcinoma (PDAC) remains a highly lethal disease in critical need of new therapeutic strategies. Here, we report that the stress-inducible 78-kDa glucose-regulated protein (GRP78/HSPA5), a key regulator of endoplasmic reticulum homeostasis and PI3K/AKT signaling, is overexpressed in the acini and PDAC of *Pdx1-Cre;Kras$^{G12D/+}$;p53$^{f/+}$* (PKC) mice as early as 2 mo, suggesting that GRP78 could exert a protective effect on acinar cells under stress, as during PDAC development. The PKC pancreata bearing wild-type *Grp78* showed detectable PDAC by 3 mo and rapid subsequent tumor growth. In contrast, the PKC pancreata bearing a *Grp78$^{f/+}$* allele (PKC78$^{f/+}$ mice) expressing about 50% of GRP78 maintained normal sizes during the early months, with reduced proliferation and suppression of AKT, S6, ERK, and STAT3 activation. Acinar-to-ductal metaplasia (ADM) has been identified as a key tumor initiation mechanism of PDAC. Compared with PKC, the PKC78$^{f/+}$ pancreata showed substantial reduction of ADM as well as pancreatic intraepithelial neoplasia-1 (PanIN-1), PanIN-2, and PanIN-3 and delayed onset of PDAC. ADM in response to transforming growth factor α was also suppressed in ex vivo cultures of acinar cell clusters isolated from mouse pancreas bearing targeted heterozygous knockout of *Grp78* (*c78$^{f/+}$*) and subjected to 3D culture in collagen. We further discovered that GRP78 haploinsufficiency in both the PKC78$^{f/+}$ and *c78$^{f/+}$* pancreata leads to reduction of epidermal growth factor receptor, which is critical for ADM initiation. Collectively, our studies establish a role for GRP78 in ADM and PDAC development.

glucose-regulated protein 78 | GRP78 | pancreatic ductal adenocarcinoma | acinar-to-ductal metaplasia | *Kras*

Pancreatic ductal adenocarcinoma (PDAC) remains one of the deadliest diseases with limited therapeutic options and an overall 5-y survival rate of <10%; therefore, identification of targetable key players in tumor initiation as well as tumor maintenance is urgently needed (1). PDAC is believed to arise from a range of preneoplastic mucinous lesions with ductal morphology, pancreatic intraepithelial neoplasia (PanIN) being the most common in humans (2). About 90% of PDAC contains activating mutations of *KRAS* whereas 50–75% contain mutations in *Tp53* (1). Mutationally activated oncogenic KRAS signals through the PI3K-PDK1-AKT pathway and the canonical mitogen-activated protein kinase pathway via RAF-MEK1/2-ERK1/2, as well as via positive feedback activation of receptor tyrosine kinases engaged by autocrine and paracrine stimuli (3). Although the histological appearance of PDAC suggests a ductal cell of origin, accumulating evidence reveals that PDAC originates primarily through transdifferentiation of acinar cells into ductal cells in a process referred to as acinar-to-ductal metaplasia (ADM), although centroacinar cells and pancreas precursor cells could also give rise to PDAC (2, 4, 5). To study PDAC, a pancreatic cancer mouse model mimicking human PDAC has been established using the pancreatic and duodenal homeobox 1 promoter-driven Cre-recombinase (*Pdx1-Cre*) to conditionally activate the *Kras lox-stop-lox G12D* allele and delete one allele of *p53*. Upon Cre activation, the *lox-stop-lox* cassette is removed and the oncogenic *Kras^{G12D}* allele is activated (6). This mouse model, *Pdx1-Cre;Kras$^{G12D/+}$;p53$^{f/+}$* (referred to as the "PKC mice"), and other closely related mouse models of pancreatic cancer result in PanIN at 2 mo of age, which is rapidly followed by PDAC development (7, 8). Given the difficulty in targeting KRAS directly, the PKC model provides an invaluable platform to uncover novel determinants that are critical for pancreatic carcinogenesis.

The 78-kDa glucose-regulated protein (GRP78), also referred to as BiP/HSPA5, is a major endoplasmic reticulum (ER) chaperone with antiapoptotic properties and a key regulator of ER stress signaling (9). Cancer cells are subjected to ER stress due to intrinsic factors such as genetic mutations, altered metabolism, and hyperproliferation as well as extrinsic factors in the tumor microenvironment including oxygen and nutrient deprivation (10–13). A characteristic of pancreatic cancer is the formation of a dense stroma termed "desmoplastic reaction" that induces vascular collapse leading to severe hypoxia and glucose deprivation (1). As an adaptive measure, cancer cells turn on the unfolded protein response (UPR) (10, 11, 13). ER stress induction of GRP78 in

Significance

***KRAS* is mutated in more than 90% of pancreatic adenocarcinoma (PDAC). Despite its well-known role in cancer, development of drugs directly targeting *KRAS* has been unfruitful, underscoring the critical need to identify novel therapeutic targets. This study provides evidence that haploinsufficiency of a single cellular protein, GRP78, although having no harmful effect on the normal pancreas, is sufficient to impede *Kras*-driven pancreatic tumorigenesis in a genetically engineered mouse model. This study also establishes a role of GRP78 in acinar-to-ductal metaplasia, which is regarded as a precursor to PDAC development.**

Author contributions: J.S., D.P.H., G.Z., and A.S.L. designed research; J.S., D.P.H., G.Z., and D.F.R. performed research; D.F.R., A.K., P.S.G., and S.G. contributed new reagents/analytic tools; J.S., D.P.H., G.Z., D.F.R., S.G., L.D., and A.S.L. analyzed data; and J.S., D.P.H., D.F.R., L.D., and A.S.L. wrote the paper.

The authors declare no conflict of interest.

This article is a PNAS Direct Submission. D.A.C. is a guest editor invited by the Editorial Board.

[1]Present address: Centre of New Technologies, University of Warsaw, 02-097 Warsaw, Poland.

[2]To whom correspondence should be addressed. Email: amylee@usc.edu.

This article contains supporting information online at www.pnas.org/lookup/suppl/doi:10.1073/pnas.1616060114/-/DCSupplemental.

www.pnas.org/cgi/doi/10.1073/pnas.1616060114

cancer cells represents a major prosurvival response, suppressing apoptosis while promoting proliferation and invasiveness (14). Recently, it was discovered that ER stress can actively promote cell-surface localization of GRP78 (15), where it assumes coreceptor functions with cell-surface protein partners in regulating signal transduction pathways, including PI3K/AKT/S6 activation (16–19). Although homozygous knockout of *Grp78* results in embryonic lethality, heterozygous *Grp78* mice expressing an ~50% level of GRP78 are viable and phenotypically normal (20). The creation of targeted heterozygous knockout of *Grp78* in various organs revealed that although it has a minimal effect on organ development and function, it exerts a profound suppressive effect in both solid and blood tumors notably driven by loss of the *Pten* tumor suppressor gene (14, 21, 22). Despite these advances, the mechanistic involvement of GRP78 in oncogenic mutant *KRAS*-driven cancers is just emerging.

GRP78 has been identified as a biomarker in human PDAC by several independent studies. A high level of GRP78 was detected by mass spectrometry imaging and immunohistochemistry (IHC), as well as proteomic and tissue microarray profiling of microdissected pancreatic cancer nests and was associated with poor prognosis and shorter overall survival (23–25). Furthermore, GRP78 was up-regulated in ductal structures of both human and murine ADM and PDAC lesions and colocalized with activated AKT on the cell surface (26). In human PDAC cell lines, knockdown of GRP78 or treatment of the cells with anti-GRP78 agents resulted in decreased proliferation, invasion, viability, and chemoresistance, suggesting that suppression of GRP78 could represent a novel approach to combat human mutant *KRAS*-driven PDAC (14, 25, 27, 28).

These interesting developments prompted us to investigate the effect of GRP78 haploinsufficiency on pancreatic tumorigenesis using the PKC mouse model and the underlying molecular mechanisms. Our studies established a critical role for GRP78 in mutant *Kras*-driven pancreatic tumorigenesis and uncovered a previously unidentified requirement of GRP78 in acinar-to-ductal transdifferentiation considered to be a precursor of pancreatic neoplasia. Proliferation and elevation of EGFR and oncogenic signaling pathways observed in the PKC mice were also suppressed by GRP78 haploinsufficiency. Our studies support GRP78 as a therapeutic target in combating mutant *KRAS*-driven pancreatic tumorigenesis.

Results

Up-Regulation of GRP78 in Pancreatic Acinar and Ductal Cells of PKC Mice. Pancreatic cancer cells could experience a high level of ER stress due to increased proliferation driven by the *Kras* activation and desmoplasia leading to tissue hypovascularity. Consistent with this notion, we observed general, sustained up-regulation of GRP78 in the acinar cells of the PKC mice compared with control mice, which lack the *Pdx1-Cre* transgene. This increase was detected as early as 2 mo (Fig. 1*A*), suggesting that GRP78 could be exerting a protective effect on the acinar cells under stress associated with PDAC development. In the pancreatic cancer lesions, GRP78 expression was highly elevated, in contrast to the low level of GRP78 expression in the ductal structures of control mice (Fig. 1*B*).

To investigate the impact of GRP78 on pancreatic tumorigenesis, *Pdx1-Cre;Kras*$^{G12D/+}$*; p53*$^{f/+}$*;Grp78*$^{f/+}$ mice (referred to as PKC78$^{f/+}$) were generated to create GRP78 pancreatic haploinsufficiency (Fig. S1*A*). Genotyping of pancreatic genomic DNA by PCR confirmed the genotypes of the respective mouse cohorts and further validated the presence of the recombined *Kras*^{G12D} allele in the PKC and the PKC78$^{f/+}$ mice harboring the *Pdx-1 Cre* allele (Fig. 1*C*). Littermates lacking the *Pdx1-Cre* transgene served as controls.

As expected, the PKC pancreata showed abnormal masses by 3 mo, which rapidly increased in size, whereas the appearance and size of PKC78$^{f/+}$ pancreata remained normal during the early months, with no tumor being macroscopically detectable before 5 mo (Fig. 1*D*). The weight of the pancreata in the three genotypes paralleled their gross morphology (Fig. 1*E*). IHC analysis of the pancreatic sections confirmed a reduced GRP78 level in both acinar and ductal cells in the PKC78$^{f/+}$ pancreata compared with PKC pancreata that were sustained at least up to 5 mo (Fig. 1*F*). Quantification of GRP78 IHC staining in the ductal structures showed that, although staining of GRP78 in the normal ducts of the control mice was minimal, the large increase of GRP78 staining in the malignant lesions of PKC mice was reduced by about 70% in the PKC78$^{f/+}$ mice (Fig. 1*G*). The level of phosphorylated eIF2α (p-eIF2α), a marker of ER stress-induced translational arrest (10), was also highly elevated in the malignant lesions of the PKC pancreata but not in the PKC78$^{f/+}$ pancreata (Fig. 1*H*). Interestingly, the expression of another ER chaperone, GRP94, was readily detected in the normal ducts of the control mice (Fig. S2*A*). In contrast to other tissues where GRP94 was up-regulated to compensate for GRP78 haploinsufficiency (29), the level of GRP94 in the ductal structures was similar in the PKC and PKC78$^{f/+}$ mice (Fig. S2*A*). CCAAT-enhancer binding protein homologous protein (CHOP), a marker of ER stress-induced onset of apoptosis (10), was not detected in the control, PKC, or PKC78$^{f/+}$ pancreata (Fig. S2*B*).

Suppression of *Kras*-Driven Pancreatic Tumorigenesis by *Grp78* Heterozygosity. Histological sections of pancreata from 2- to 4-mo-old control, PKC, and PKC78$^{f/+}$ mice are shown in Fig. 2. No evidence of malignant or premalignant lesion was found in any of the control mice, from which representative normal ducts are shown. The PKC pancreata showed extensive PanIN-1, characterized by mucinous differentiation with no nuclear atypia, as early as 2 mo of age and showed invasive adenocarcinoma at 3 and 4 mo. An example of a solid, sarcomatoid pattern of ductal adenocarcinoma is shown from a 3-mo-old PKC mouse whereas the tumor shown from the 4-mo-old mouse with this genotype formed distorted small acini in a dense stroma. Sarcomatoid elements were identified in only two tumors, both from PKC mice. Although PanIN-1 was also seen in 2-mo-old PKC78$^{f/+}$ mice, ADM, characterized by ducts confined to acinar portions in which at least one cell shows intracellular secretions, was the predominant abnormality in this group. At 3 mo, PKC78$^{f/+}$ mice exhibited PanIN-1 and an occasional focus of PanIN-2 characterized by some degree of nuclear atypia in at least some epithelial cells. PanIN-3, characterized by more severe nuclear as well as architectural atypia, was occasionally detected in the PKC78$^{f/+}$ mice at 3 and 4 mo (Fig. 2).

Quantification of the ratio of histologically normal pancreatic areas over total pancreatic areas at different ages up to 5 mo showed that all PKC78$^{f/+}$ pancreata retained 80–100% areas of normal acinar tissue up to 4 mo, whereas age-matched PKC pancreata were more aggressively and progressively replaced by metaplasia, PanIN, and PDAC (Fig. 3*A*). By 5 mo, whereas half of the PKC78$^{f/+}$ pancreata were histologically normal in over 80% of their respective total areas, all PKC pancreata showed 40–90% replacement with metaplasia, PanIN, or PDAC. Quantification of the different types of lesions showed that at 3 mo the PKC78$^{f/+}$ pancreata exhibited significantly lower incidences of ADM (P = 0.003), low-grade neoplasia (PanIN-1) (P = 0.033), and combined high-grade neoplasia (PanIN-2, -3) and PDAC (P = 0.026), compared with the PKC pancreata (Fig. 3*B*). Notably, at 3 mo PDAC was detected only in the PKC mice and PKC78$^{f/+}$ pancreata showed only minimal PanIN-3. In agreement with the reduced tumor volumes and incidences, PKC78$^{f/+}$ mice showed a trend toward a prolonged life span compared with PKC mice (P = 0.035, one-sided log-rank test, Fig. S3); interestingly, this trend was observed predominantly in the males (P = 0.038, one-sided log-rank test) and not in the females (P = 0.39, one-sided log-rank test, Fig. 3*C*).

Suppression of Proliferation and Oncogenic Signaling in PKC78$^{f/+}$ Pancreata. In agreement with reduced tumor involvement in the PKC78$^{f/+}$ pancreata as indicated by morphological and

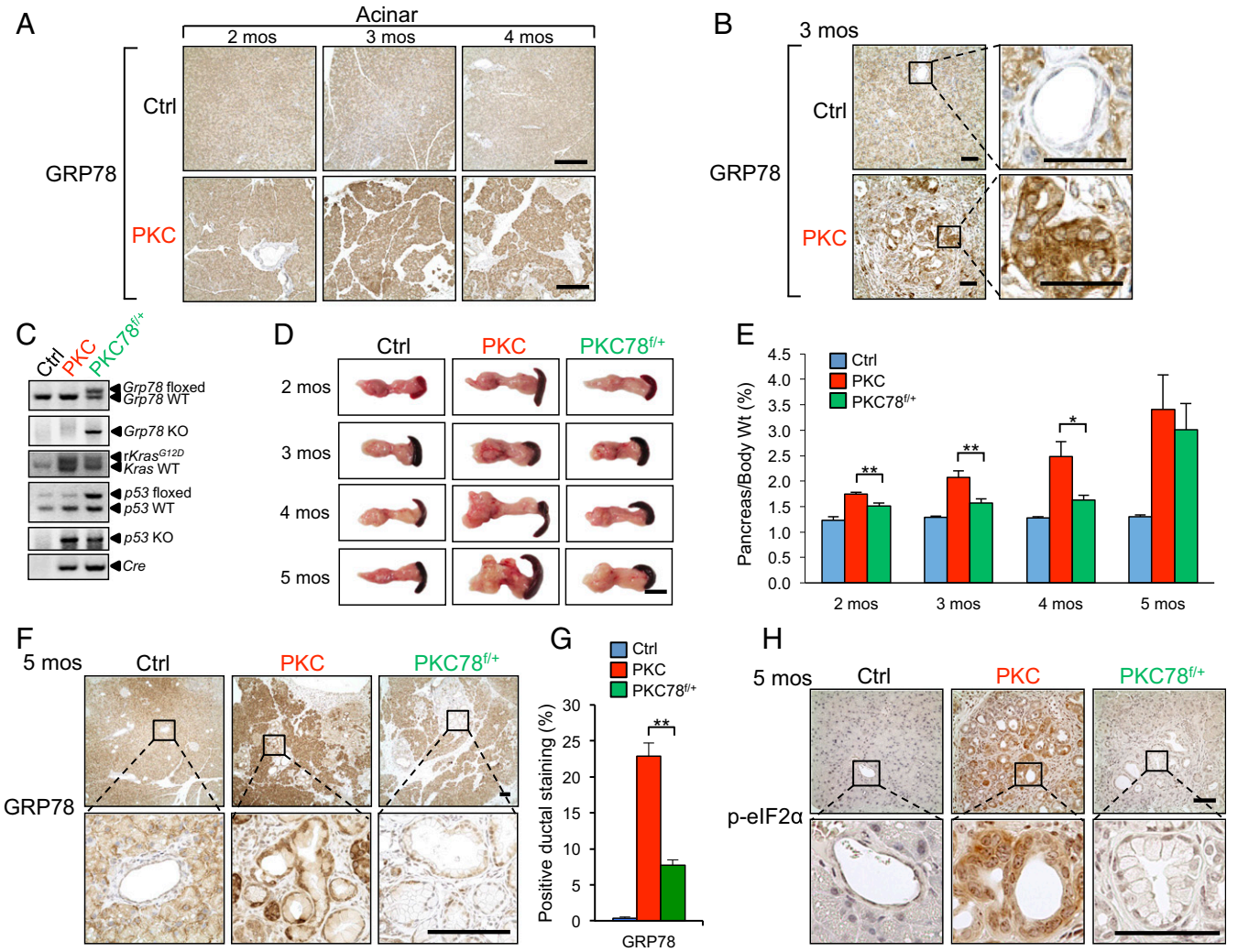

Fig. 1. Comparative analysis of the PKC and PKC78$^{f/+}$ pancreata. (*A*) IHC of GRP78 in control (Ctrl) and PKC pancreata at 2, 3, and 4 mo. (Scale bar, 200 μm.) (*B*) IHC of GRP78 in the indicated 3-mo-old pancreata with enlarged views of ductal/pancreatic tumor lesions. (Scale bar, 100 μm.) (*C*) Representative PCR genotyping of indicated alleles from pancreatic genomic DNA. *rKras*^{G12D} represents the recombined allele. (*D*) Representative gross anatomy of pancreata of the indicated genotypes at the indicated age. (Scale bar, 1 cm.) (*E*) Percentage of pancreas weight over body weight in the indicated genotypes at the indicated age. The numbers for the Ctrl, PKC, and PKC78$^{f/+}$ mice: at 2 mo (n = 10, 10, and 9, respectively); at 3 mo (n = 18, 15, and 11, respectively); at 4 mo (n = 15, 8, and 8, respectively); and at 5 mo (n = 12, 8, and 8, respectively). The data are presented as mean ± SE; *P < 0.05 and **P < 0.01. (*F*) IHC of GRP78 of pancreata of the indicated genotypes at 5 mo with enlarged views of ductal/pancreatic tumor lesions. (Scale bar, 50 μm.) (*G*) Quantification of GRP78 staining from *F* in ductal structures represents average staining of the sampled images ± SE; **P < 0.01. The number of images that were randomly selected for quantification are the following: Ctrl (n = 10), PKC (n = 15), and PKC78$^{f/+}$ (n = 15). For each genotype, the images were obtained from two to three mice. (*H*) IHC of p-eIF2α of pancreata of the indicated genotypes at 5 mo with enlarged views of ductal/pancreatic tumor lesions. (Scale bar, 50 μm.)

histological parameters, IHC of epithelial cell-marker pan-cytokeratin (panCK) (Fig. S4*A*) and activated myofibroblast marker α-smooth muscle actin (α-SMA), characteristics of pancreatic tumors, showed a decrease of both markers in PKC78$^{f/+}$ pancreata compared with PKC pancreata (Fig. 4*A*). Signaling pathways including PI3K/S6, ERK, STAT3, and β-catenin have been reported to be activated in PDAC (3, 30, 31). As expected, these pathways were prominently up-regulated in the PKC pancreata (Fig. 4*A*). The PKC78$^{f/+}$ pancreata displayed reduction in S6 activation in both ductal and acinar cells (Fig. 4*A* and Fig. S4*B*). ERK activation, STAT3 activation, and β-catenin level were also reduced in the PKC78$^{f/+}$ pancreata. Quantification of the staining levels of each of the markers in multiple pancreatic sections of each of the three genotypes confirmed a significant reduction of these oncogenic signaling pathways in the PKC78$^{f/+}$ pancreata (Fig. 4*B*). Furthermore, Western blotting of protein lysates from isolated pancreatic acinar clusters provided biochemical confirmation of a 60% reduction in AKT activation in PKC78$^{f/+}$ pancreata compared with PKC pancreata (Fig. 4*C*).

Tumor growth is regulated by a balance between proliferation and apoptosis. Proliferation marker Ki67 showed a two- to threefold reduction in PKC78$^{f/+}$ compared with PKC pancreata in both acinar and ductal cells (Fig. 4*D* and Fig. S5*A*). IHC showed minimal staining for cleaved caspase-3, a biomarker of apoptosis, in both PKC and PKC78$^{f/+}$ pancreata (Fig. S5*B*). Collectively, these results imply that the suppression of tumorigenesis by pancreatic GRP78 haploinsufficiency is driven by reduction of mutant *Kras*-mediated proliferation and oncogenic signaling, rather than by increased apoptosis.

Reduction of Transdifferentiation from Acinar-to-Ductal Cells in PKC78$^{f/+}$ Pancreata. ADM has been identified as a primary mechanism for initiation of PDAC (5, 32). Given the elevated GRP78 level in

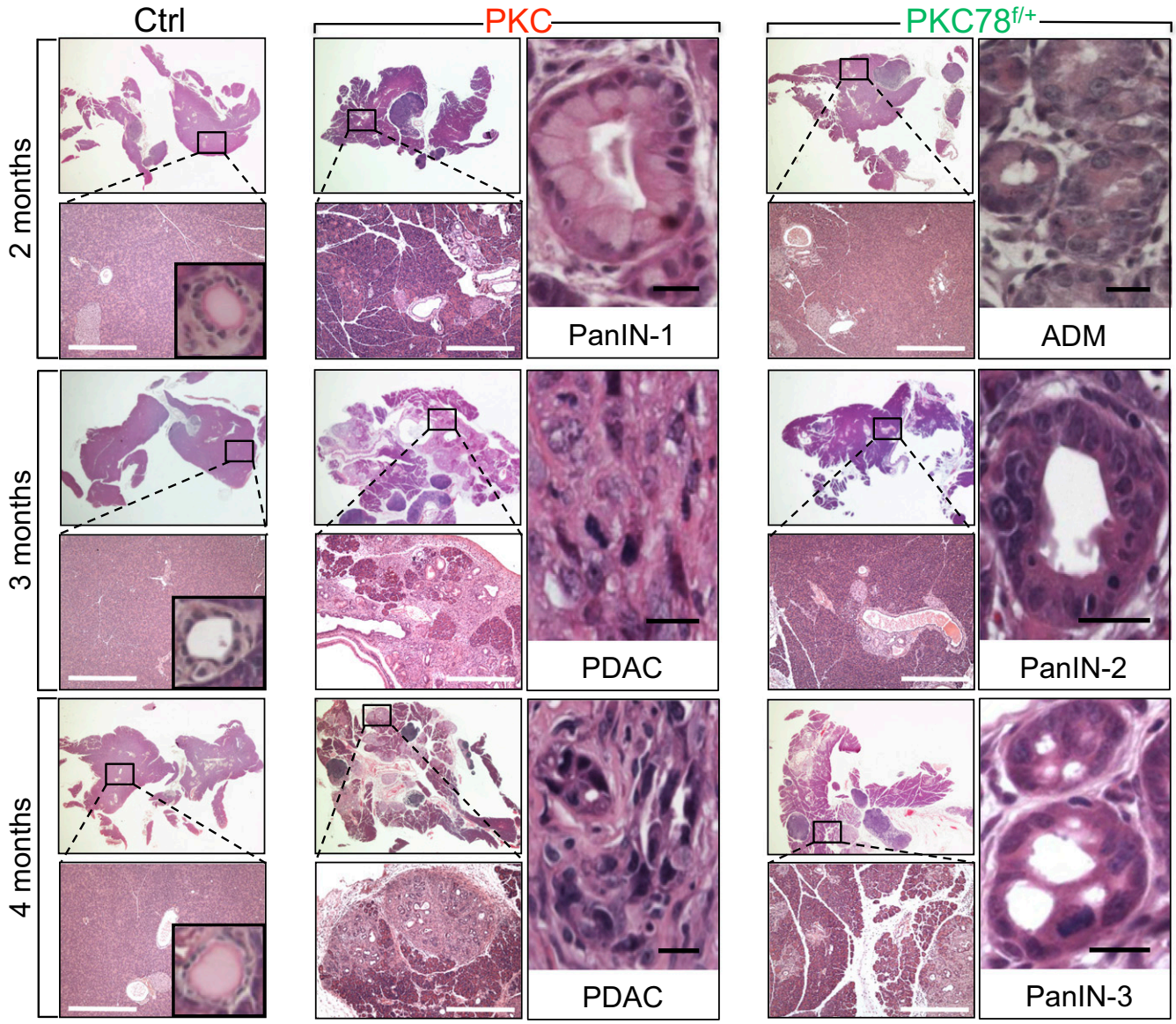

Fig. 2. Histological examination of pancreata. Representative H&E staining of pancreata of the indicated genotypes at the indicated ages. For the control mice, *Insets* show enlarged views of representative pancreatic ducts. For the PKC and PKC78$^{f/+}$ mice, enlarged views of examples of premalignant (ADM) and malignant lesions (PanIN-1, -2, and-3) and PDAC are shown. (Scale bars: white bars, 500 μm; black bars, 15 μm.)

PKC acinar cells, its up-regulation may play a role in pancreatic ADM subjected to oncogenic stress. ADM is characterized by acinar clusters staining positive for both acinar (amylase) and ductal (pan-cytokeratin) markers. The number of cellular clusters coexpressing panCK and amylase was substantially reduced in PKC78$^{f/+}$ pancreata (Fig. 5*A*). Quantification by immunofluorescence indicated a 65% reduction in panCK positivity and an 80% reduction in ADM in PKC78$^{f/+}$ pancreata compared with PKC (Fig. 5*B*), implying that GRP78 haploinsufficiency could lead to suppression of ADM during the initiation of PDAC.

EGFR signaling has been reported to play an important role in ADM in *KRAS*-induced pancreatic tumorigenesis (33). As EGFR is a client protein of GRP78 in the ER (34, 35), we examined whether GRP78 haploinsufficiency affected EGFR expression, thus providing an explanation for the reduction of ADM in the PKC78$^{f/+}$ pancreas. Indeed, PKC pancreata expressed about fivefold more EGFR than control pancreata, and this increase was reduced by 60% in the PKC78$^{f/+}$ pancreata based on Western blot analyses (Fig. 5*C*). In other cell types, such as human head and neck cancer cells (scc-351) and in human embryonic kidney HEK-293T cells, specific shRNA knockdown of GRP78 also led to substantial reduction in EGFR levels (Fig. S6*A*).

***Grp78* Heterozygous Pancreas Is Phenotypically Normal but Exhibits Deficient ADM Induced by Transforming Growth Factor α.** To directly address whether GRP78 is required for pancreatic ADM, we studied the impact of GRP78 haploinsufficiency on pancreatic ductal formation during normal development or transdifferentiation from acinar cells stimulated by transforming growth factor α (TGFα), which binds to its receptor EGFR and activates downstream signals including RAS and AKT (3). We created the *Pdx1-Cre;Grp78*$^{f/+}$ mice (referred to below as *c78*$^{f/+}$) with targeted heterozygous knockout of *Grp78* in the pancreas. The genotypes of *c78*$^{f/+}$ and its sibling control mice without the *Pdx1-Cre* allele were confirmed by PCR of tail genomic DNA (Fig. S1*B*). The size and weight of control and *c78*$^{f/+}$ pancreata were similar at 2–9 mo (Fig. S7 *A* and *B*). Histological analysis of pancreatic sections stained with H&E showed similar morphological features between

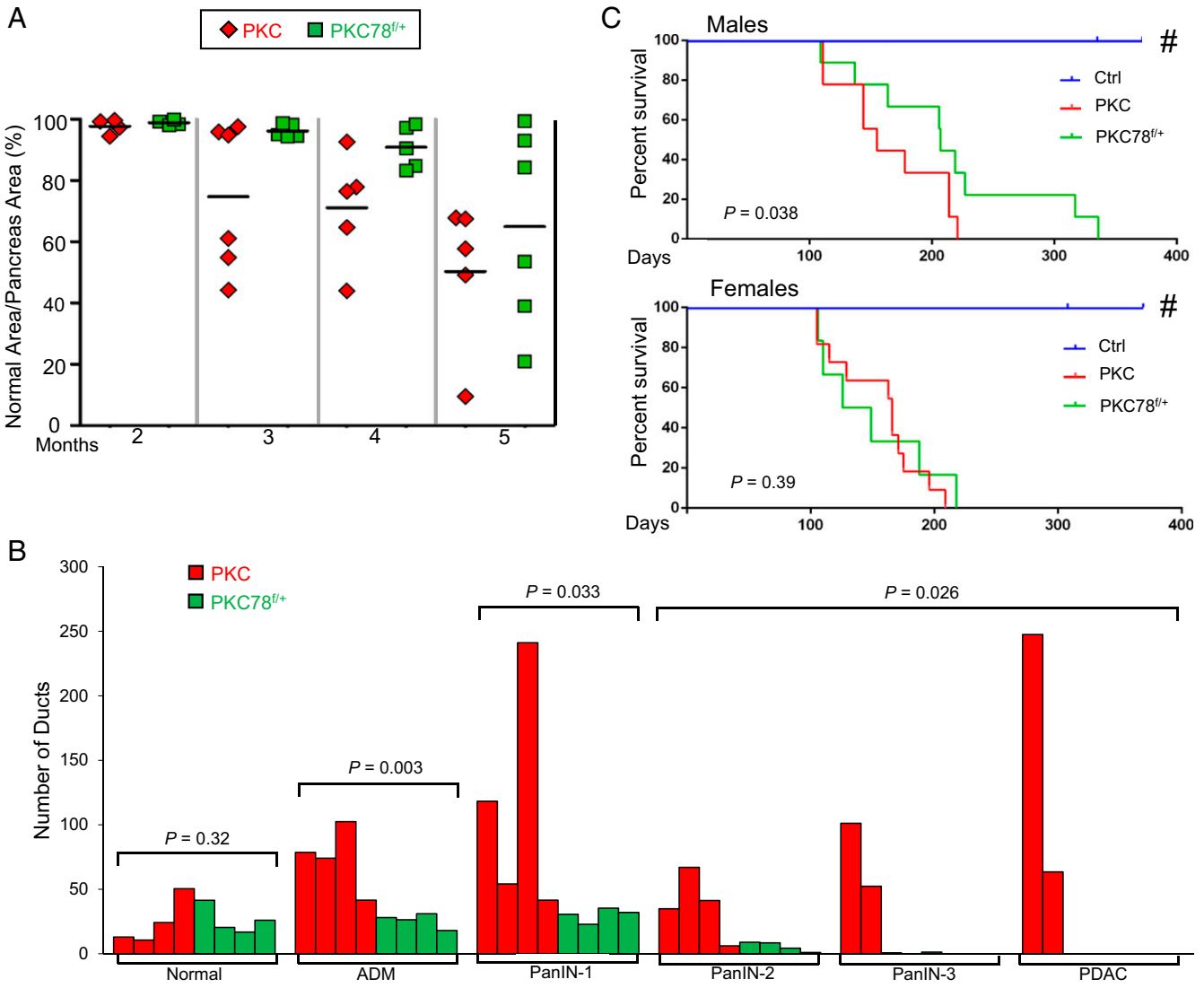

Fig. 3. Reduced pancreatic tumorigenesis in PKC78$^{f/+}$ pancreata. (*A*) Percentage of total pancreatic area showing a normal appearance in PKC and PKC78$^{f/+}$ mice at the indicated ages. (*B*) Quantification of ADM, PanIN-1, -2, -3, and PDAC in pancreata from 3-mo-old PKC ($n = 4$) and PKC78$^{f/+}$ ($n = 4$) mice. Each bar represents the total number of ducts in one mouse. Each feature was determined from histological examination of entire single longitudinal sections through the entire pancreas of individual PKC (red) and PKC78$^{f/+}$ (green) mice. The *P* values compare the two genotypes under each bracket. (*C*) Kaplan–Meier survival curve of male control (Ctrl) ($n = 10$), PKC ($n = 9$), and PKC78$^{f/+}$ ($n = 9$) mice (*Upper*) and female Ctrl ($n = 10$), PKC ($n = 11$), and PKC78$^{f/+}$ ($n = 6$) mice (*Lower*). $P = 0.038$ for male mice and $P = 0.39$ for female mice, one-sided log-rank test. The "#" symbol represents more control (Ctrl) mice living beyond 400 d, which are not displayed on the graph.

control and *c78*$^{f/+}$ pancreata (Fig. S7*C*). An approximate 50% reduction of GRP78 in the *c78*$^{f/+}$ pancreata compared with control was confirmed by IHC; staining with ductal marker panCK indicated normal ductal morphology (Fig. S7*D*). Quantification of the number of ducts in control and *c78*$^{f/+}$ pancreata showed no difference between the two genotypes (Fig. S7*E*). For comparison, we also created *c78*$^{f/f}$ mice with homozygous deletion of the *Grp78* allele. The *c78*$^{f/f}$ pancreata showed extensive fat infiltration with poorly developed acinar cells (Fig. S7*F*) and were significantly smaller (Fig. S7*G*). In contrast to the *c78*$^{f/+}$ mice, which exhibited normal glucose tolerance comparable to control mice, the *c78*$^{f/f}$ mice showed impaired glucose tolerance (Fig. S7*H*).

Because the *c78*$^{f/+}$ mice display normal development of both exocrine and endocrine pancreas, this model was chosen to determine the effect of GRP78 haploinsufficiency on growth-factor–stimulated ADM. Pancreatic acinar clusters were isolated from control and *c78*$^{f/+}$ mice, subjected to 3D explant culture in collagen, and stimulated with TGFα (Fig. 6*A*). The *c78*$^{f/+}$ acinar cells exhibited fewer ductal structures, confirmed by decreased panCK-positive clusters, compared with control on day 3 (Fig. 6*B*). Quantification of ducts formed in vitro showed an approximate 50% reduction in ductal structures derived from *c78*$^{f/+}$ acinar cells compared with control, and an approximate 35% reduction in panCK-positive cells on day 3 (Fig. 6*C*). The acinar clusters undergoing ADM were characterized by coexpression of both acinar (amylase) and ductal (panCK) markers in the same cell cluster. Corresponding to reduced ductal formation, *c78*$^{f/+}$ acinar clusters showed reduced ADM compared with control as evidenced by decreased panCK expression and sustained amylase expression (Fig. 6*D*).

Next we isolated acinar clusters from the pancreas and confirmed by Western blot analysis that GRP78 level was reduced by about 50% in *c78*$^{f/+}$ acinar clusters compared with control (Fig. 6*E*). Biochemical analysis revealed shortly following culture,

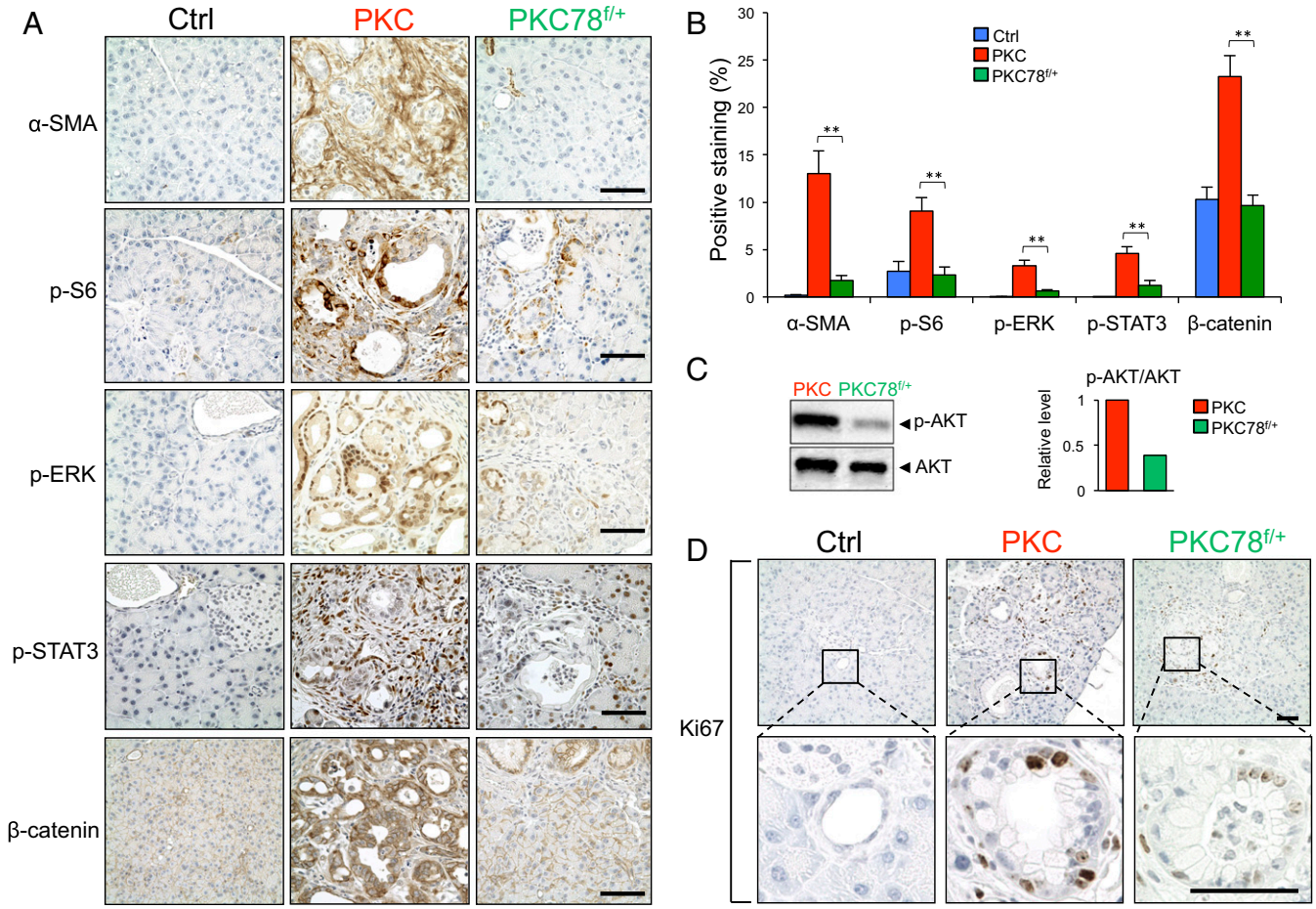

Fig. 4. Decreased oncogenic signaling and proliferation in the PKC78$^{f/+}$ pancreata. (*A*) IHC of α-SMA, p-S6 (Ser235/236), p-ERK (Thr202/Tyr204), p-STAT3 (Tyr705), and β-catenin of the pancreata of the indicated genotypes at 3 mo. (Scale bar, 100 μm.) (*B*) Quantification of α-SMA, p-S6 (Ser235/236), p-ERK (Thr202/Tyr204), p-STAT3 (Tyr705), and β-catenin staining from *A*. The values represent the average staining of the sampled areas ± SE; $^{**}P < 0.01$. Quantification of α-SMA, p-S6, and β-catenin, the cytoplasm of which was stained, and that of p-ERK and p-STAT3, the nuclei of which were stained, is shown. Number of images that were randomly chosen to be quantified are the following: α-SMA–control (Ctrl) ($n = 15$); PKC ($n = 10$); PKC78$^{f/+}$ ($n = 15$); p-S6–Ctrl ($n = 15$); PKC ($n = 17$); PKC78$^{f/+}$ ($n = 15$); p-ERK–Ctrl ($n = 15$); PKC ($n = 16$); PKC78$^{f/+}$ ($n = 17$); p-STAT3–Ctrl ($n = 15$); PKC ($n = 22$); PKC78$^{f/+}$ ($n = 20$); β-Catenin–Ctrl ($n = 10$); PKC ($n = 15$); and PKC78$^{f/+}$ ($n = 17$). For Ctrl, at least two mice were examined, and for PKC and PKC78$^{f/+}$, three mice were analyzed. (*C*) Western blot analysis of p-AKT (Ser473) and AKT levels of isolated acinar cells from the PKC and PKC78$^{f/+}$ mice. Relative levels of p-AKT normalized to AKT are shown in bar graph. (*D*) IHC of Ki67 of the pancreata of the indicated genotypes at 3 mo with enlarged views of ductal lesions below. (Scale bar, 50 μm.)

compared with control, *c78*$^{f/+}$ acinar cells showed reduced basal levels of p-AKT and p-ERK but similar levels of p-STAT3 normalized to AKT, ERK, and STAT3, respectively (Fig. 6*F*). Starting at day 2, TGFα induced AKT and ERK activation but not STAT3 in the control acinar cell clusters. Interestingly, *c78*$^{f/+}$ acinar cells showed some increase in p-AKT on day 2, and, by day 3, the level of p-AKT had reached that of the control. In contrast, p-ERK was suppressed in the *c78*$^{f/+}$ acinar cells from day 0 to day 3, and the ratio of p-STAT3 over total STAT3 level was similar in both genotypes from day 0 to day 3 (Fig. 6*F*). Thus, these signaling pathways were differentially regulated in the *c78*$^{f/+}$ acinar in these ex vivo settings. We further examined the status of EGFR expression in these acinar cells. Consistent with suppression of EGFR levels in the PKC78$^{f/+}$ pancreata, EGFR level in the *c78*$^{f/+}$ acinar cells was also reduced compared with control (Fig. S6*B*). Thus, in both mouse models, GRP78 haploinsufficiency suppresses EGFR expression.

Discussion

KRAS is commonly mutated in various cancers. In pancreatic cancer, *KRAS* is mutated in more than 90% of PDAC (1). The recent observation that activating *KRAS* mutations were present in >90% of pancreatic PanIN-1 lesions suggests that the acquisition of *KRAS* mutations likely precedes the formation of these precursor lesions (36). In addition to its role in tumor initiation, oncogenic KRAS is also required for PDAC maintenance (37). Despite its well-known role in cancer, development of drugs targeting KRAS directly has been unfruitful, underscoring the need for alternative approaches (3). The UPR is an adaptive measure for cells to overcome ER stress, which can be pronounced in cancer cells with limited vasculature. In human PDAC tumor resected specimens, expression of the ER stress markers GRP78, GRP94, and spliced XBP-1 has been reported (26, 38, 39). Here, we used the well-established PKC mouse model bearing oncogenic *Kras*^{G12D} and *p53* heterozygosity to interrogate the role of GRP78 in pancreatic tumorigenesis and the underlying mechanisms. IHC analysis showed that pancreatic tumors in PKC mice also expressed elevated levels of GRP78 and eIF2α phosphorylation, suggestive of ER stress. GRP78 is an essential chaperone, and we showed that homozygous deletion of both alleles in the pancreas led to abnormal pancreatic development, fat infiltration, and glucose intolerance. Given that *Grp78* heterozygosity does not affect normal pancreatic function, we created the PKC78$^{f/+}$ mice so that GRP78 haploinsufficiency could be concomitantly induced with

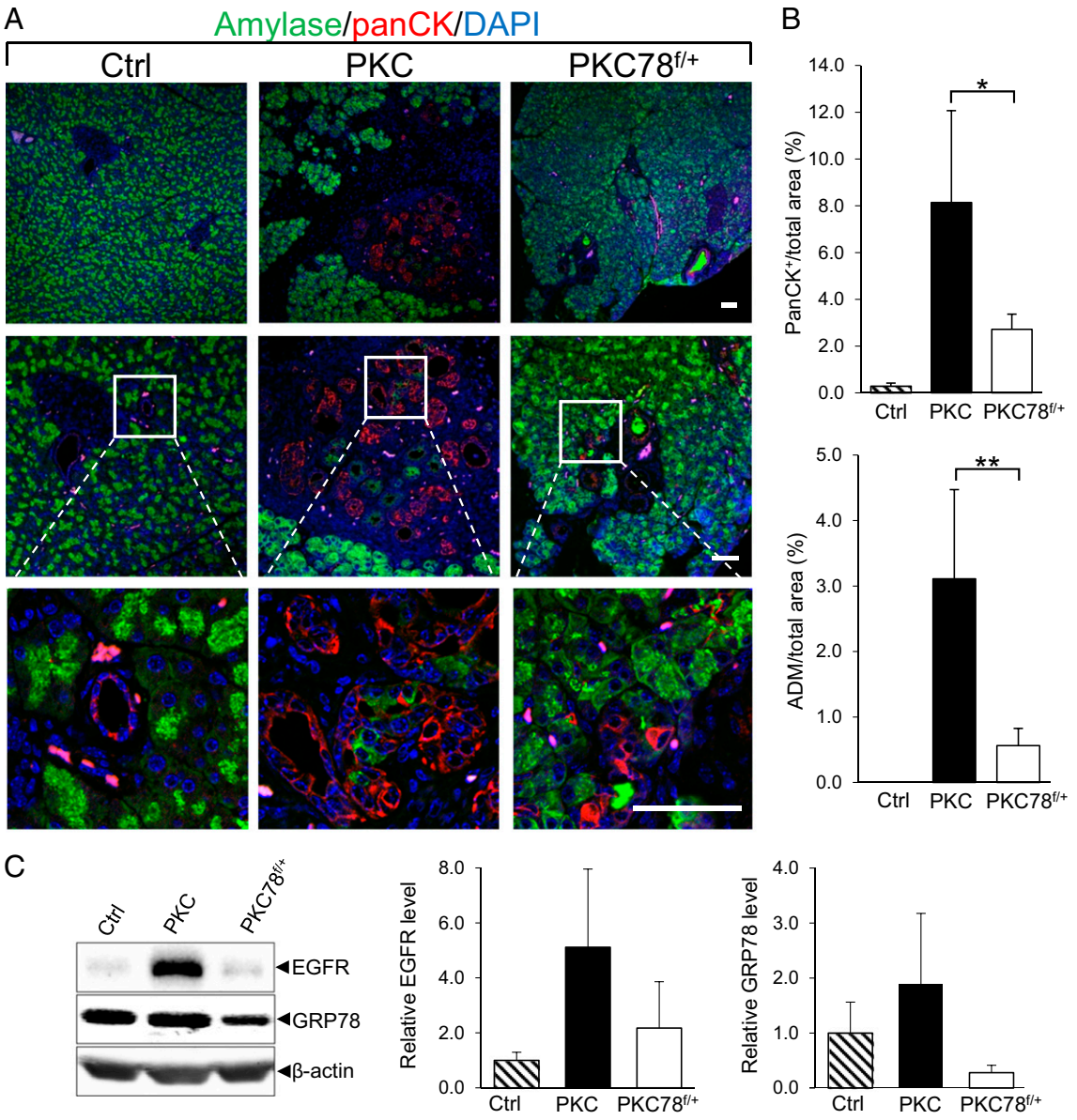

Fig. 5. Decreased acinar-to-ductal metaplasia in PKC78$^{f/+}$ pancreata. (*A*) Double IF staining for amylase (green) and panCK (red) in pancreata with the indicated genotypes at 3 mo with enlarged views of the indicated areas. Nuclei were stained with DAPI (blue). (Scale bar, 50 μm.) (*B*) Quantification of the percentage of panCK-positive and ADM-positive areas (coexpression of amylase and panCK in the same cluster) in the pancreata of the indicated genotypes: Control (Ctrl) (two mice, 5 images/mice), PKC (two mice, 11 images/mice), and PKC78$^{f/+}$ (2 mice, 11 images/mice). The data are presented as mean ± SE; *P < 0.05 and **P < 0.01. (*C*) Western blot analysis of EGFR and GRP78 levels in pancreatic tissue lysates from the indicated genotypes (n = 3 for each genotype). Relative levels of EGFR and GRP78 normalized to β-actin are shown in bar graphs.

activation of the oncogenic mutant genes. Comparative analysis of the PKC, PKC78$^{f/+}$, and *c78*$^{f/+}$ pancreata led to observations that shed insights on GRP78 function in the mouse pancreas subjected to mutant *Kras*-induced tumorigenesis.

First, in the PKC mice, GRP78 was highly elevated not only in PDAC but also in acinar cells. As professional secretory cells, acinar cells are highly dependent on ER functions and are particularly susceptible to ER stress (40). Interestingly, acinar cells respond to stress such as pancreatitis through activation of regenerative mechanisms that initiate ADM, a process that replaces damaged acinar cells with duct-like structures (41). Although the relationship between ER stress and ADM is not well understood, a recent report suggests that ER stress resulting from perturbation of basal autophagy via loss of ATG7 is associated with spontaneous activation of ADM in a mouse model (42). ADM is critical for the initiation of pancreatic tumorigenesis (5, 32). In the PKC acinar cells, GRP78 was highly elevated, suggesting that it could play a role in ADM under oncogenic stress. Here, using a genetically engineered mouse model, we report substantial reduction of ADM in the PKC78$^{f/+}$ pancreata compared with PKC. This includes histological analysis of pancreatic tumor sections based on morphological parameters and IHC staining of acinar and ductal markers followed by quantification. Our results provide evidence that GRP78 haploinsufficiency could lead to suppression of ADM during the initiation process of PDAC. In further support of a role for GRP78 in ADM, we created the *c78*$^{f/+}$ mice, which in contrast to *c78*$^{f/f}$ mice, are phenotypically normal. Here, we showed that acinar cell explants isolated from *c78*$^{f/+}$ mice and cultured in 3D

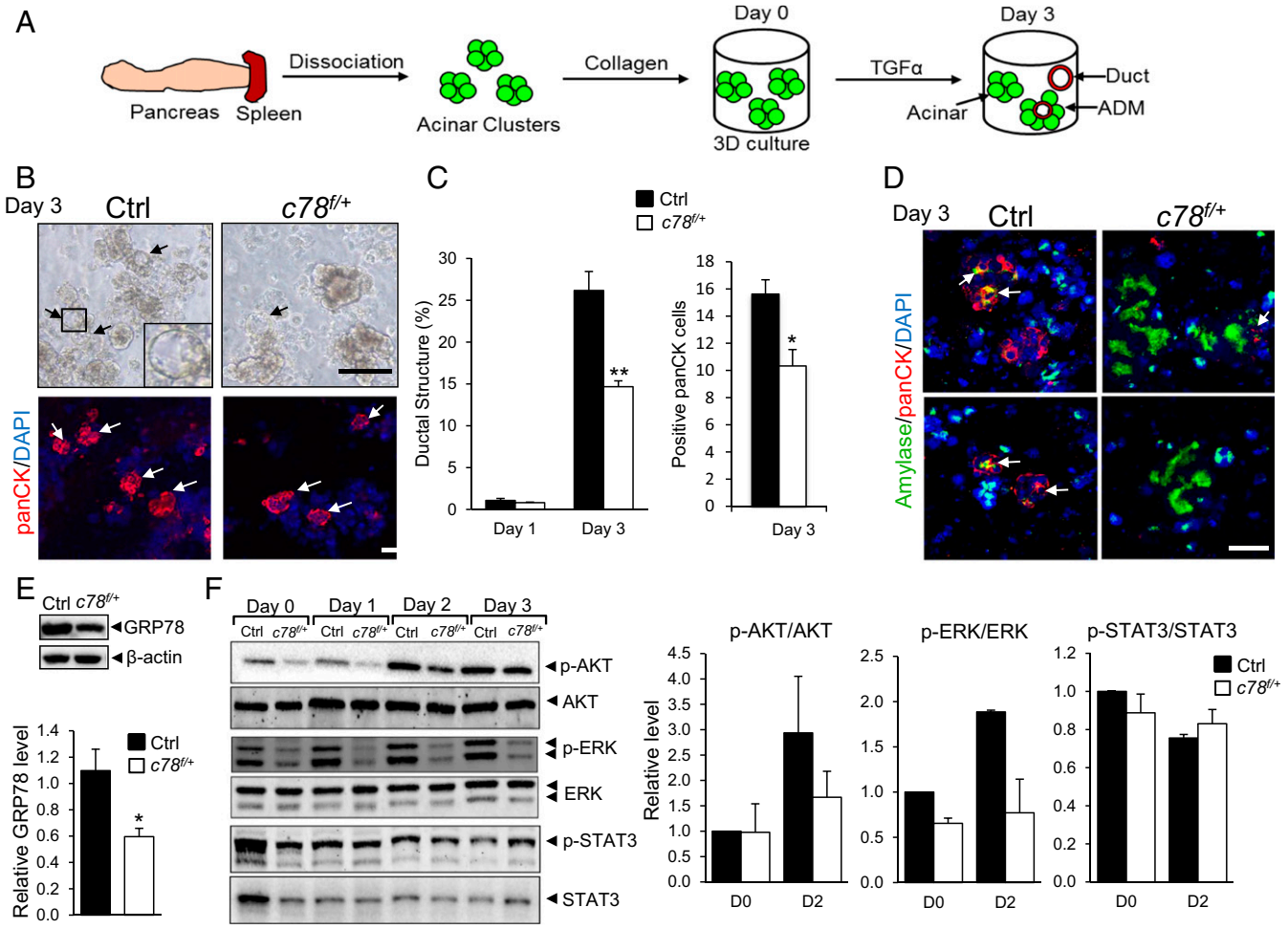

Fig. 6. Decreased TGFα-induced acinar-to-ductal transdifferentiation in explanted $c78^{f/+}$ acinar cells. (*A*) Scheme of TGFα-stimulated in vitro pancreatic acinar-to-ductal metaplasia assay following extraction of pancreatic acinar cells. (*B*) Light microscopy (*Upper*) and IF (*Lower*), with panCK stained in red and nuclei stained in blue (DAPI), of the explanted acinar cells collected from the indicated genotypes on day 3. Black arrows denote ducts and white arrows denote acinar clusters with panCK expression. (Scale bar, 50 μm.) (*C*) Quantification of the percentage of ducts in the entire acinar compartment of the indicated genotypes on days 1 and 3 and quantification of panCK-positive acinar structures of indicated genotypes on day 3. Three pairs of mice were analyzed, and for each mouse at least eight wells were examined. The data are presented as mean ± SE; $*P < 0.05$ and $**P < 0.01$. (*D*) Double IF of amylase (green) and panCK (red) of explanted acinar cell clusters of the indicated genotypes at day 3. Nuclei were stained with DAPI (blue). White arrows denote acinar clusters undergoing ADM. (Scale bar, 100 μm.) (*E*) Representative Western blot analysis of GRP78 in explanted Ctrl ($n = 3$) and $c78^{f/+}$ ($n = 3$) acinar cells with β-actin serving as loading control and quantification of band densities. The data are presented as mean ± SE; $*P < 0.05$. (*F*) Representative Western blots of p-AKT (Ser473), AKT, p-ERK (Thr202/204), ERK, p-STAT3 (Tyr705), and STAT3 of the TGFα-treated explanted Ctrl ($n = 2$) and $c78^{f/+}$ ($n = 2$) acinar cells on days 0, 1, 2, and 3. Quantification of duplicate experiments is displayed in bar graphs. The data are presented as mean ± SE.

explant in collagen matrices exhibited lower ADM following stimulation with TGFα, compared with similar explants isolated from control mice. Thus, in both PKC78$^{f/+}$ and $c78^{f/+}$ models, under either in vivo or ex vivo settings, GRP78 is required for ADM.

In the search for potential mechanisms whereby GRP78 haploinsufficiency suppresses ADM, we discovered that the level of EGFR was substantially reduced in the PKC78$^{f/+}$ and $c78^{f/+}$ mouse pancreatic cells, which also exhibited reduced ADM. Other human cells whereby the level of GRP78 was reduced by genetic knockdown of GRP78 also exhibited reduced EGFR level. Here, we observed up-regulation of EGFR in the PKC model. EGFR activity is essential for metaplastic duct formation and initiation of KRAS-induced pancreatic tumorigenesis (33). GPR78 was reported to directly complex with EGFR in the ER (34, 35) and to cooperate with activated α2-macroglobulin to facilitate the interaction between EGFR and c-Src on the cell surface (43). Thus, GRP78 could regulate the synthesis, transport, and stability of EGFR, thereby affecting its activation and downstream signaling, which impacts ADM and PDAC development.

In addition to EGFR, the PKC78$^{f/+}$ pancreata also displayed reduction in p-AKT, p-S6, p-ERK, p-STAT3, and β-catenin compared with PKC. AKT signaling is a critical axis in pancreatic initiation and maintenance. Chemical inhibition of AKT suppressed both human and murine ADM (44). Previous studies of GRP78 and *Pten*-null–induced prostate cancer and leukemia revealed that GRP78 haploinsufficiency potently suppressed AKT activation mediated by loss of PTEN in these cancers (21, 22). Subsequently, it was demonstrated that the cell-surface form of GRP78 (scGRP78) complexes with PI3K to promote phosphatidylinositol (3–5)-trisphosphate formation (18). Targeting csGRP78 with a monoclonal antibody led to suppression of AKT signaling and tumor growth (45, 46). CsGRP78 is also an obligatory binding partner for Cripto, a GPI-anchored cell-surface protein and an upstream regulator of the TGFβ pathway and of AKT (47, 48). GRP78 has been shown to costain with p-AKT in PDAC (26); thus, similar mechanisms may apply. ERK activation is also critical for ADM induction and PDAC development formation, and ERK inhibitor blocks TGFα-induced ADM (33, 49). Silencing GRP78 in

hepatocellular carcinoma cells and glioblastoma cells reduced ERK activation, suggesting a causative effect (50, 51). Reduction of GRP78 may diminish ERK activation via its effect on EGFR. It is also highly possible that GRP78 as a chaperone is needed for processing or stabilizing various client proteins required for AKT, ERK, STAT3, and β-catenin signaling, and this warrants further investigation.

In the acinar cell clusters isolated from $c78^{f/+}$ mice and cultured in 3D culture, basal levels of p-AKT and p-ERK were reduced compared with control, and the reduced level of p-ERK remained 3 d following TGFα stimulation. Intriguingly, in contrast to ERK, induction of p-AKT was observed in the isolated $c78^{f/+}$ cells 2 d after treatment with TGFα. A possible explanation is that, as AKT and ERK can be stimulated by multiple pathways, in these ex vivo settings, ERK stimulation by TGFα is highly dependent on GRP78 levels in the isolated acinar clusters, whereas other mechanisms could compensate for GRP78 haploinsufficiency to activate AKT. This is in agreement with a published report that GRP78 induced a strong activation of ERK in endothelial cells and a weak activation of AKT (52). In these ex vivo cultures, TGFα did not stimulate p-STAT3 activation, and the ratio of p-STAT3 to total STAT3 level remained unchanged between $c78^{f/+}$ and control cells.

GRP78 haploinsufficiency in the PKC model, although having no effect on apoptosis, slowed tumor proliferation, correlating with lower levels of ADM, PanIN-1, -2, and -3 and delaying the onset of PDAC compared with PKC mice. In following the survival of these mouse cohorts, we noted a trend toward a prolonged life span of the $PKC78^{f/+}$ mice compared with the PKC mice, and interestingly, the prolonged survival was observed predominantly in the male. Consistent with this observation, in our limited analysis, we noted that the male $PKC78^{f/+}$ mice showed a trend toward smaller tumor volumes compared with female mice at 5 mo. Larger cohort sizes in future studies are needed to clarify the significance of these observations. Although the reasons for the gender difference remain to be determined, we also observed a differential survival response between the $Grp78^{+/-}$ male and female mice following chemotherapy (53), and others have also reported gender differences in tumor severity and survival in other mouse cancer models (54–56).

In summary, our studies uncovered previously unidentified roles of GRP78 in acinar-to-ductal transdifferentiation and provide proof-of-principle that GRP78 haploinsufficiency is sufficient to suppress PDAC development and oncogenic signaling in *Kras*-driven pancreatic cancer. Furthermore, in human PDAC cell lines, GRP78 has been reported to promote proliferation, migration, invasion, viability, and chemoresistance (14, 25, 27, 28). Thus, the utility of inhibitors of GRP78 expression in combating PDAC and chemoresistance merits further investigation.

Materials and Methods

Mice. The $c78^{f/+}$ mice were generated by breeding the *Pdx1-Cre* mice with the $Grp78^{f/f}$ mice (20) (Fig. S1*A*). The PKC and the $PKC78^{f/+}$ mice were generated by breeding the $Kras^{G12D/+}$;$p53^{f/f}$ mice with *Pdx1-Cre*;$Grp78^{f/+}$ mice (Fig. S1*A*). Genotyping of DNA from the mouse tail or pancreas was performed by PCR. Primers for detection of the *Pdx1-Cre* and *floxed* or knockout alleles for *Grp78* and *p53* were described previously (21, 57). To determine if recombination of the $Kras^{G12D}$ *lox-stop-lox* cassette occurred, DNA was extracted from pancreas and PCR was performed following the protocol described from the Jacks Lab (https://jacks-lab.mit.edu/protocols/genotyping/kras_cond). Primer 1, 5′-GTCTTTCCCCAGCACAGTGC-3′, and primer 2, 5′-CTCTTGCCTACGCCACCAGCTC-3′, were used to detect the recombined or the wild-type alleles. All protocols for animal use and euthanasia were reviewed and approved by the University of Southern California Institutional Animal Care and Use Committee.

Tissue Processing and Histology. Both male and female mice were euthanized and the pancreata were isolated. Collected samples were either frozen in liquid nitrogen for biochemical analysis or fixed in 10% zinc formalin (Sigma-Aldrich) for tissue analysis. Paraffin-embedded tissues were sectioned at 4 μm.

Immunohistochemistry. Immunostaining of the paraffin-embedded tissue sections was performed as described previously (21). Tissue sections were incubated at 4 °C overnight with primary antibodies. For IHC, the following antibodies were used: GRP78 (1:500, Abcam #ab108613), pan-cytokeratin (1:50, Abcam #ab9377), p-eIF2α (1:50, Cell Signaling #3398), p-S6 (Ser235/236, 1:200, Cell Signaling #4856), p-ERK (Thr202/Tyr204, 1:200, Cell Signaling #4370), p-STAT3 (Tyr705, 1:50, Cell Signaling #9145), Ki67 (1:200, Thermo Fisher Scientific #RM-9106), β-catenin (1:200, Santa Cruz Biotechnology #sc-7199) and α-SMA (1:2,000, Sigma-Aldrich #A2547). For immunofluorescence (IF) staining, the following antibodies were used: Amylase (1:50, Santa Cruz Biotechnology #sc-12821) and pan-cytokeratin (1:50, Abcam #ab9377). Immunofluorescence was visualized using a Zeiss LSM 510 confocal microscope with LSM 510 Version 4.2 SP1 acquisition software, and the images were analyzed with ZEN lite imaging software (Zeiss) and Adobe Photoshop CS5.

Quantification of Immunohistochemical Staining. All slides evaluated for IHC 3,3′-diaminobenzidine staining of the pancreas were performed using the histogram function of the Adobe Photoshop CS5 Imaging software. This software function can specifically mine for staining intensities in various cell compartments such as the nucleus and cytoplasm as well as in the ductal structures. All of the sampled images that were randomly selected and analyzed were of a fixed size.

Primary Acinar Cell Explant Culture. Primary acinar cell clusters were prepared as described (58) and were seeded in collagen into 48-well plates, cultured, and treated with recombinant human TGFα (50 ng/mL, Novoprotein) and immunostained as described (59).

Glucose Tolerance Test. Glucose tolerance was tested as previously described (60). Mouse tail blood was measured for glucose by the OneTouch Ultra System (Lifescan) at indicated time points after i.p. injection of glucose (1 mg/g body weight) in 2-mo-old mice that had fasted overnight.

Protein Extraction and Immunoblot Analysis. The cell lysates were prepared and subjected to 10% or 12% SDS/PAGE and Western blot analysis as described (61). The following primary antibodies were used: GRP78 (1:1,000, BD Biosciences #610978), EGFR (1:1,000, Cell Signaling #4267), STAT3 (1:1,000, BD Biosciences #610190), β-actin (1:2,000, Sigma-Aldrich #A5316), p-ERK (Thr202/Tyr204, 1:1,000, Cell Signaling #9106), ERK (1:1,000, Cell Signaling #9102), p-STAT3 (Tyr705, 1:1,000, Cell Signaling #9145), p-AKT (Ser473, 1:1,000, Cell Signaling #9271), and AKT (1:1,000, Cell Signaling #9272). The secondary antibodies were as follows: horseradish peroxidase conjugate goat anti-mouse, anti-rabbit, and anti-rat antibodies (1:1,000, Santa Cruz Biotechnology #sc-2005, #sc-2004, #sc-2006); goat anti-mouse IRDye 800CW (1:7,500, LI-COR Biosciences); and goat anti-rabbit IRDye 680RD (1:7,500, LI-COR Biosciences) secondary antibodies. Protein levels were visualized and quantitated by either ChemiDoc XRS+ Imager (Bio-Rad Laboratories) or LICOR Odyssey (LI-COR Biosciences).

Statistical Analysis. Statistical analysis was performed with either two-tailed Student's *t* test or a log-rank (Mantel–Cox) test for survival data. For comparing the numbers of ducts with various features, the log transformation was used before analysis, and the Satterwaite correction was used to adjust for unequal variances due to the intrinsic heterogeneity of the PKC model. For both the survival and the ductal analyses, our a priori hypothesis was that $PKC78^{f/+}$ mice would survive longer and have fewer ducts with abnormal features, and hence the *P* values are one-sided.

ACKNOWLEDGMENTS. We thank Ben Stanger, Gangning Liang, Bangyan Stiles, Qilong Ying, Wan-Ting Chen, Ren Liu, Hai-Yun Yen, and Suhn K. Rhie for providing biological specimens, reagents, and helpful discussions; the University of Southern California Norris Comprehensive Cancer Center Biostatistics Core for assistance in data analysis; the Translational Pathology Core and the University of Southern California School of Pharmacy Histology Laboratory for tissue processing; and the University of Southern California Research Center for Liver Diseases Cell and the Tissue Imaging Core for the use of microscopy. The work was supported by National Institutes of Health Grants R21 CA179273, R01 CA027607 (to A.S.L.), and R01 CA133117 (to L.D.) and by the Julia Stearns Dockweiler Foundation (A.S.L.). The University of Southern California Norris Comprehensive Cancer Center Biostatistics and Translational Pathology Cores were supported by NIH Grant P30 CA014089, and the University of Southern California Research Center for Liver Diseases Cell and Tissue Imaging Core was supported by NIH Grant P30 DK048522.

1. Hidalgo M (2010) Pancreatic cancer. *N Engl J Med* 362:1605–1617.
2. Ying H, et al. (2016) Genetics and biology of pancreatic ductal adenocarcinoma. *Genes Dev* 30:355–385.
3. Eser S, Schnieke A, Schneider G, Saur D (2014) Oncogenic KRAS signalling in pancreatic cancer. *Br J Cancer* 111:817–822.
4. Stanger BZ, et al. (2005) Pten constrains centroacinar cell expansion and malignant transformation in the pancreas. *Cancer Cell* 8:185–195.
5. Kopp JL, et al. (2012) Identification of Sox9-dependent acinar-to-ductal reprogramming as the principal mechanism for initiation of pancreatic ductal adenocarcinoma. *Cancer Cell* 22:737–750.
6. Jackson EL, et al. (2001) Analysis of lung tumor initiation and progression using conditional expression of oncogenic K-ras. *Genes Dev* 15:3243–3248.
7. Rhim AD, et al. (2012) EMT and dissemination precede pancreatic tumor formation. *Cell* 148:349–361.
8. Herreros-Villanueva M, Hijona E, Cosme A, Bujanda L (2012) Mouse models of pancreatic cancer. *World J Gastroenterol* 18:1286–1294.
9. Ni M, Lee AS (2007) ER chaperones in mammalian development and human diseases. *FEBS Lett* 581:3641–3651.
10. Luo B, Lee AS (2013) The critical roles of endoplasmic reticulum chaperones and unfolded protein response in tumorigenesis and anticancer therapies. *Oncogene* 32: 805–818.
11. Clarke HJ, Chambers JE, Liniker E, Marciniak SJ (2014) Endoplasmic reticulum stress in malignancy. *Cancer Cell* 25:563–573.
12. Wang M, Kaufman RJ (2014) The impact of the endoplasmic reticulum protein-folding environment on cancer development. *Nat Rev Cancer* 14:581–597.
13. Urra H, Dufey E, Avril T, Chevet E, Hetz C (2016) Endoplasmic reticulum stress and the hallmarks of cancer. *Trends Cancer* 2:252–262.
14. Lee AS (2014) Glucose-regulated proteins in cancer: Molecular mechanisms and therapeutic potential. *Nat Rev Cancer* 14:263–276.
15. Zhang Y, Liu R, Ni M, Gill P, Lee AS (2010) Cell surface relocalization of the endoplasmic reticulum chaperone and unfolded protein response regulator GRP78/BiP. *J Biol Chem* 285:15065–15075.
16. Ni M, Zhang Y, Lee AS (2011) Beyond the endoplasmic reticulum: Atypical GRP78 in cell viability, signalling and therapeutic targeting. *Biochem J* 434:181–188.
17. Gonzalez-Gronow M, Selim MA, Papalas J, Pizzo SV (2009) GRP78: A multifunctional receptor on the cell surface. *Antioxid Redox Signal* 11:2299–2306.
18. Zhang Y, et al. (2013) Cancer cells resistant to therapy promote cell surface relocalization of GRP78 which complexes with PI3K and enhances PI(3,4,5)P3 production. *PLoS One* 8:e80071.
19. Sato M, Yao VJ, Arap W, Pasqualini R (2010) GRP78 signaling hub a receptor for targeted tumor therapy. *Adv Genet* 69:97–114.
20. Luo S, Mao C, Lee B, Lee AS (2006) GRP78/BiP is required for cell proliferation and protecting the inner cell mass from apoptosis during early mouse embryonic development. *Mol Cell Biol* 26:5688–5697.
21. Fu Y, et al. (2008) Pten null prostate tumorigenesis and AKT activation are blocked by targeted knockout of ER chaperone GRP78/BiP in prostate epithelium. *Proc Natl Acad Sci USA* 105:19444–19449.
22. Wey S, et al. (2012) Inducible knockout of GRP78/BiP in the hematopoietic system suppresses Pten-null leukemogenesis and AKT oncogenic signaling. *Blood* 119: 817–825.
23. Cui Y, et al. (2009) Proteomic profiling in pancreatic cancer with and without lymph node metastasis. *Int J Cancer* 124:1614–1621.
24. Djidja MC, et al. (2009) MALDI-ion mobility separation-mass spectrometry imaging of glucose-regulated protein 78 kDa (Grp78) in human formalin-fixed, paraffin-embedded pancreatic adenocarcinoma tissue sections. *J Proteome Res* 8:4876–4884.
25. Niu Z, et al. (2015) Elevated GRP78 expression is associated with poor prognosis in patients with pancreatic cancer. *Sci Rep* 5:16067.
26. Hill R, et al. (2012) Cell intrinsic role of COX-2 in pancreatic cancer development. *Mol Cancer Ther* 11:2127–2137.
27. Gifford JB, et al. (2016) Expression of GRP78, master regulator of the unfolded protein response, increases chemoresistance in pancreatic ductal adenocarcinoma. *Mol Cancer Ther* 15:1043–1052.
28. Cerezo M, et al. (2016) Compounds triggering ER stress exert anti-melanoma effects and overcome BRAF inhibitor resistance. *Cancer Cell* 29:805–819.
29. Ye R, et al. (2010) Grp78 heterozygosity promotes adaptive unfolded protein response and attenuates diet-induced obesity and insulin resistance. *Diabetes* 59:6–16.
30. Morris JP, IV, Wang SC, Hebrok M (2010) KRAS, Hedgehog, Wnt and the twisted developmental biology of pancreatic ductal adenocarcinoma. *Nat Rev Cancer* 10: 683–695.
31. Corcoran RB, et al. (2011) STAT3 plays a critical role in KRAS-induced pancreatic tumorigenesis. *Cancer Res* 71:5020–5029.
32. Wei D, et al. (2016) KLF4 is essential for induction of cellular identity change and acinar-to-ductal reprogramming during early pancreatic carcinogenesis. *Cancer Cell* 29:324–338.
33. Ardito CM, et al. (2012) EGF receptor is required for KRAS-induced pancreatic tumorigenesis. *Cancer Cell* 22:304–317.
34. Cai B, Tomida A, Mikami K, Nagata K, Tsuruo T (1998) Down-regulation of epidermal growth factor receptor-signaling pathway by binding of GRP78/BiP to the receptor under glucose-starved stress conditions. *J Cell Physiol* 177:282–288.
35. Liu G, Shang Y, Yu Y (2006) Induced endoplasmic reticulum (ER) stress and binding of over-expressed ER specific chaperone GRP78/BiP with dimerized epidermal growth factor receptor in mammalian cells exposed to low concentration of N-methyl-N′-nitro-N-nitrosoguanidine. *Mutat Res* 596:12–21.
36. Kanda M, et al. (2012) Presence of somatic mutations in most early-stage pancreatic intraepithelial neoplasia. *Gastroenterology* 142:730–733; e739.
37. Collins MA, et al. (2012) Oncogenic Kras is required for both the initiation and maintenance of pancreatic cancer in mice. *J Clin Invest* 122:639–653.
38. Romero-Ramirez L, et al. (2009) X box-binding protein 1 regulates angiogenesis in human pancreatic adenocarcinomas. *Transl Oncol* 2:31–38.
39. Pan Z, Erkan M, Streit S, Friess H, Kleeff J (2009) Silencing of GRP94 expression promotes apoptosis in pancreatic cancer cells. *Int J Oncol* 35:823–828.
40. Ye R, et al. (2010) Grp78 heterozygosity regulates chaperone balance in exocrine pancreas with differential response to cerulein-induced acute pancreatitis. *Am J Pathol* 177:2827–2836.
41. Morris JP, IV, Cano DA, Sekine S, Wang SC, Hebrok M (2010) Beta-catenin blocks Kras-dependent reprogramming of acini into pancreatic cancer precursor lesions in mice. *J Clin Invest* 120:508–520.
42. Antonucci L, et al. (2015) Basal autophagy maintains pancreatic acinar cell homeostasis and protein synthesis and prevents ER stress. *Proc Natl Acad Sci USA* 112: E6166–E6174.
43. Zhao S, et al. (2015) The role of c-Src in the invasion and metastasis of hepatocellular carcinoma cells induced by association of cell surface GRP78 with activated α2M. *BMC Cancer* 15:389.
44. Eser S, et al. (2013) Selective requirement of PI3K/PDK1 signaling for Kras oncogene-driven pancreatic cell plasticity and cancer. *Cancer Cell* 23:406–420.
45. Liu R, et al. (2013) Monoclonal antibody against cell surface GRP78 as a novel agent in suppressing PI3K/AKT signaling, tumor growth, and metastasis. *Clin Cancer Res* 19: 6802–6811.
46. Lin YG, et al. (2015) Targeting the glucose-regulated protein-78 abrogates Pten-null driven AKT activation and endometrioid tumorigenesis. *Oncogene* 34:5418–5426.
47. Shani G, et al. (2008) GRP78 and Cripto form a complex at the cell surface and collaborate to inhibit transforming growth factor beta signaling and enhance cell growth. *Mol Cell Biol* 28:666–677.
48. Spike BT, et al. (2014) CRIPTO/GRP78 signaling maintains fetal and adult mammary stem cells ex vivo. *Stem Cell Rep* 2:427–439.
49. Shi G, et al. (2013) Maintenance of acinar cell organization is critical to preventing Kras-induced acinar-ductal metaplasia. *Oncogene* 32:1950–1958.
50. Li H, et al. (2012) Knockdown of glucose-regulated protein 78 decreases the invasion, metalloproteinase expression and ECM degradation in hepatocellular carcinoma cells. *J Exp Clin Cancer Res* 31:39.
51. Zhang LH, Yang XL, Zhang X, Cheng JX, Zhang W (2011) Association of elevated GRP78 expression with increased astrocytoma malignancy via Akt and ERK pathways. *Brain Res* 1371:23–31.
52. Kern J, et al. (2009) GRP-78 secreted by tumor cells blocks the antiangiogenic activity of bortezomib. *Blood* 114:3960–3967.
53. Lee AS, et al. (2017) Effects of prolonged GRP78 haploinsufficiency on organ homeostasis, behavior, cancer and chemotoxic resistance in aged mice. *Sci Rep* 7:40919.
54. Lee SM, et al. (2016) The effect of sex on the azoxymethane/dextran sulfate sodium-treated mice model of colon cancer. *J Cancer Prev* 21:271–278.
55. Cherukuri DP, et al. (2014) Targeted Cox2 gene deletion in intestinal epithelial cells decreases tumorigenesis in female, but not male, ApcMin/+ mice. *Mol Oncol* 8: 169–177.
56. Holzenberger M, et al. (2003) IGF-1 receptor regulates lifespan and resistance to oxidative stress in mice. *Nature* 421:182–187.
57. Jackson EL, et al. (2005) The differential effects of mutant p53 alleles on advanced murine lung cancer. *Cancer Res* 65:10280–10288.
58. Gout J, et al. (2013) Isolation and culture of mouse primary pancreatic acinar cells. *J Vis Exp* (78):e50514.
59. Sawey ET, Johnson JA, Crawford HC (2007) Matrix metalloproteinase 7 controls pancreatic acinar cell transdifferentiation by activating the Notch signaling pathway. *Proc Natl Acad Sci USA* 104:19327–19332.
60. Ye R, et al. (2011) Inositol 1,4,5-trisphosphate receptor 1 mutation perturbs glucose homeostasis and enhances susceptibility to diet-induced diabetes. *J Endocrinol* 210: 209–217.
61. Li J, et al. (2008) The unfolded protein response regulator GRP78/BiP is required for endoplasmic reticulum integrity and stress-induced autophagy in mammalian cells. *Cell Death Differ* 15:1460–1471.